Journal of Advanced Zoology
ISSN: 0253-7214
Volume 45 Issue 2 Year 2024 Page 580:592

# In-silico approaches of *Abrus precatorius* compounds as potential drug inhibitors against alpha-amylase protein (4gqr).

**Neha Verma[1*], Indra Prasad Tripathi[2] & Vandana Pathak[3]**

*[1*]Research Scholar, Department of physical Sciences, Mahatma Gandhi Chitrakoot Gramodaya Vishwavidyalaya, Chitrakoot, Satna (M.P.),) 485334, nehavermabari@gmail.com,*
*[2]Dean, Faculty of science and environment, Mahatma Gandhi Chitrakoot Gramodaya Vishwavidyalaya, Chitrakoot, Satna (M.P.), 485334, tripathi.ip@gmail.com,*
*[3]Associate professor, Department of physical sciences, Mahatma Gandhi Chitrakoot Gramodaya Vishwavidyalaya, Chitrakoot, Satna (M.P.) 485334*

***Corresponding Author:** Neha Verma*
*Email: nehavermabari@gmail.com*

***Article History***

Received: 06-01-2024
Revised: 20-01-2024
Accepted: 05-02-2024



***Abstract***

T2DM is characterized by high blood glucose levels and can result in significant consequences such as nephropathy, neuropathy, retinopathy, and cardiovascular disease. Inhibiting the digestion of dietary carbohydrates is one of the treatment options for managing postprandial hyperglycemia in T2DM. 95% patient have type II diabetes mellitus. Although many synthetic drugs have been identified against pancreatic a-amylase. These medications have side effects, and new medications are being developed to address these issues. Managing diabetes without side effects is a significant challenge. This study tested 83 active constituent derived from the plant *Abrus precatorius* against the human pancreatic a-amylase using in-silico computational approaches such as molecular docking and molecular dynamics simulation approaches. Schr€odinger, a drug discovery package with modules applicable for molecular docking, protein-ligand interaction analysis, molecular dynamics studies. Six active constituent, namely, the Vitexin (-10.6kcal/mol), delphinidin-3-5,diglucoside(-10.5kcal/mol,), abrusin(-9.18kcal/mol), taxifolin-3-glucoside (-8.83 kcal/mol) , pelargonidin3-glucoside (-8.72 kcal/mol), and Quercetin (-8.22 kcal/mol ). All the docking score more negative than the control ligand, i.e. Myricetin (–7.3kcal/mol). The molecular dynamics analysis suggested that top two docked compounds, it showed considerable stability within the protein's active site. As a result, Both compounds found in this work are proposed as promising antidiabetic possibilities and should be evaluated further in vitro and in vivo.

***Keywords: Diabetes mellitus, Alpha-amylase, Abrus precatorius***

## 1. Introduction:

Diabetes mellitus (DM) is a metabolic syndrome defined by chronic hyperglycemia caused by dysregulated glucose metabolism caused by abnormalities in pancreatic-cell activity[1]. Diabetes Mellitus (DM) is becoming more common across all populations worldwide on a daily basis. According to a research by the International Diabetes Federation (2011), there are currently 366 million people who have diabetes, and that number is expected to rise to 552 million by the year 2030. Adults globally were estimated to have 171 million cases of Type 2 Diabetes Mellitus in 2000, but by 2015, that number has increased to 415 million[2]. Diabetes is the most prevalent endocrine condition. Approximately 5% of diabetic people have type I diabetes, while 95% have type II diabetes mellitus[3]. T2DM is characterized by high blood glucose levels and can result in significant consequences such as nephropathy, neuropathy, retinopathy, and cardiovascular disease. Inhibiting the digestion of dietary carbohydrates is one of the treatment options for managing postprandial hyperglycemia in T2DM[4]. Therefore, reducing postprandial hyperglycemia is a therapeutic strategy for the treatment of diabetes. This can be accomplished by inhibiting enzymes that hydrolyze carbohydrates, such as alpha amylase and alpha glucosidase. Alpha amylase and alpha glucosidase are crucial enzymes in the breakdown of carbohydrates. Long chain carbohydrates are broken down by alpha amylase, while starch and disaccharides are converted to glucose by alpha glucosidase. They assist in intestinal absorption and act as the primary digestive enzymes. The development of lead medications for the treatment of diabetes may focus on alpha amylase inhibitor[5]. Currently, a number of medications, including biguanides and sulponyl ureas, are available to treat diabetic mellitus. These medications have side effects, and new medications are being developed to address these issues. Managing diabetes without side effects is a significant challenge. The need for new, more effective anti-diabetic medications, especially those with fewer side effects than alpha-amylase inhibitor, is great[3]. The demand for new, more potent anti-diabetic medications is great, especially those with less side effects like alpha-amylase inhibitors. Natural products are also well-known sources for the development of novel bioactive chemicals that can act as scaffolds for the creation of new medications, including new anti-diabetic ones[6]. Many medicinal plants are reported to be useful in diabetes. Several reports have highlighted the traditional uses of *Abrus precatorius* in the treatment and management of diabetes mellitus. *Abrus precatorius* is a valuable plant for its diabetic, nephronectins, neuroprotectants, analgesics, and other medicinal properties. *A. precatorius* is rich in a variety of chemical components, including root, seed, and leaves[7]. In this study, the active catalytic site of the pancreatic a-amylase and intestinal alpha-glucosidase has been targeted for identifying potential antidiabetic drug molecules. The six active compounds (Vitexin, delphinidin-3-5,diglucoside, abrusin, taxifolin-3-glucoside, pelargonidin3-glucoside, and Quercetin) were identified from eighty three *Abrus precatorius* active constituent based on their docking score. The dynamic stability of best two docked poses containing the target protein alpha-amylase and the ligands was analyzed using molecular dynamics (MD) simulation.

## 2. Material and Method:

### 2.1 Collection of protein and ligand for insilico study

The three-dimensional 3D structure of Pancreatic human alpha-amylase protein (PDB ID: 4GQR) in complex with myricetin. This structure contains the alpha-amylase main protease resolved using the X-ray diffraction technique at 1.20 Å resolution. It consists of a single polypeptide chain 'A' with a sequence length of 496 amino acids. The binding sites of protein interaction with its native ligand are $Trp^{59}$, $Gln^{63}$, $Asp^{197}$, and $Glu^{233}$. Respectively was retrieved as a receptor downloaded from the RCSB Protein Data Bank[8] (https://www.rcsb.org/,). The compounds used in this study for molecular docking against the proteins catalytic site were active compounds derived from the plant *Abrus precatorius*. A total of 83 active compounds were retrieved from a *Abrus precatorius* plant (show in Table-1) database known as IMPPAT (Indian Medicinal Plants, Phytochemistry and Therapeutics)[9] https://doi.org/10.1038/s41598-018-22631-zPubChem database from (https://pubchem.ncbi.nlm.nih.gov/) in SDF formate[10] .

**Table 1.** A List of all the active compounds derived from the plant *Abrus precatorius*, used in this study for molecular docking against human pancreatic a-amylase.

| S.N | IMPPAT | Compounds name | Pubchem ID |
|---|---|---|---|
| 1 | IMPHY012713 | Vitexin | CID:5280441, |
| 2 | IMPHY002910 | delphinidin-3-5,diglucoside | CID:25201902 |
| 3 | IMPHY004742 | Abrusin | CID:44258417 |
| 4 | IMPHY002608 | Taxifolin-3-glucoside | CID:14187089 |
| 5 | IMPHY001274 | Pelargonidin 3-glucoside | CID:443648 |
| 6 | IMPHY004619 | Quercetin | CID:5280343, |

| | | | |
|---|---|---|---|
| 7 | IMPHY004388 | Kaempferol | CID:5280863, |
| 8 | IMPHY015039 | D-Pinitol | CID:164619 |
| 9 | IMPHY002404 | Abricin | ND |
| 10 | IMPHY004718 | Abrectorin | CID:44257585, |
| 11 | IMPHY001246 | Carvacrol | CID:10364, |
| 12 | IMPHY012050 | D-Galactose | CID:6036, |
| 13 | IMPHY004187 | L-(+)-Arabinose | CID:5460291 |
| 14 | IMPHY006550 | Thymol | CID:6989 |
| 15 | IMPHY014927 | Glycyrrhizic acid | CID:14982, |
| 16 | IMPHY005985 | Precatorine | CID:54704420 |
| 17 | IMPHY012021 | Gallic acid | CID:370, |
| 18 | IMPHY007439 | 5beta-Cholanic acid | CID:92803 |
| 19 | 244 | phenylmethanol | ND |
| 20 | IMPHY014842 | Stigmasterol | CID:5280794 |
| 21 | IMPHY015116 | D-Xylose | CID:135191 |
| 22 | IMPHY011974 | 4-Hydroxycinnamic acid | CID:637542 |
| 23 | IMPHY000994 | Hypaphorine | CID:442106, |
| 24 | IMPHY008695 | Abrine | CID:160511, |
| 25 | IMPHY012402 | Campesterol | CID:173183, |
| 26 | IMPHY006300 | Cholesterol | CID:5997, |
| 27 | IMPHY016372 | 3'-Methoxyacetophenone | CID:11460 |
| 28 | IMPHY011642 | Cycloartenol | CID:92110, |
| 29 | IMPHY012058 | Linalool | CID:6549 |
| 30 | IMPHY005747 | Abrisapogenol J | CID:21594179, |
| 31 | IMPHY011888 | Abruslactone A | CID:44575701 |
| 32 | IMPHY007534 | Sophoradiol | CID:9846221 |
| 33 | IMPHY006709 | Acetyleugeno | CID:7136, |
| 34 | IMPHY012160 | alpha-Terpineol | CID:17100, |
| 35 | IMPHY006486 | Squalene | CID:638072 |
| 36 | IMPHY011619 | alpha-Amyrin | CID:73170, |
| 37 | IMPHY011882 | Cinnamaldehyde | CID:637511 |
| 38 | IMPHY015123 | alpha-Copaene | CID:70678558 |
| 39 | IMPHY004055 | Choline | CID:305 |
| 40 | IMPHY012667 | Caryophyllene oxide | CID:1742210, |
| 41 | IMPHY011396 | 4-Carvomenthenol | CID:11230 |
| 42 | IMPHY011231 | Triptotriterpenic acid A | CID:21594203 |
| 43 | IMPHY012223 | beta-Amyrin | CID:73145 |
| 44 | IMPHY011793 | (+)-gamma-Cadinene | CID:6432404, |
| 45 | IMPHY014806 | a-cubebene | CID:442359, |
| 46 | IMPHY005839 | Trigonelline | CID:5570 |
| 47 | IMPHY000633 | Methyl abrusgenate | ND |
| 48 | IMPHY011789 | Citral | CID:638011 |
| 49 | IMPHY001351 | Elemicin | CID:10248 |
| 50 | IMPHY011586 | germacrane d | CID:91723653 |
| 51 | IMPHY012147 | beta-Pinene | CID:14896 |
| 52 | IMPHY002588 | Flavylium | CID:145858 |
| 53 | IMPHY016825 | pinene-2-ol | CID:22013424 |
| 54 | IMPHY011552 | αlpha-thujene | CID:6451618 |
| 55 | IMPHY012061 | alpha-Pinene | CID:6654, |
| 56 | IMPHY012086 | Citronellal | CID:7794 |
| 57 | IMPHY011792 | gamma-Muurolene | CID:12313020 |
| 58 | IMPHY000587 | Pentacosanoic acid | CID:10468 |
| 59 | IMPHY014708 | beta-Selinene | CID:442393 |
| 60 | IMPHY011581 | alpha-Selinene | CID:10856614 |
| 61 | IMPHY011790 | Neral | CID:643779, |
| 62 | IMPHY001658 | Thymol methyl ether | CID:14104, |
| 63 | IMPHY012165 | Sabinene | CID:18818, |
| 64 | IMPHY011647 | Geranyl acetate | CID:1549026, |
| 65 | IMPHY013850 | Ethylenimine quinone | CID:95715 |
| 66 | IMPHY011761 | Humulene | CID:5281520, |
| 67 | IMPHY005618 | Germacrene B | CID:5281519 |
| 68 | IMPHY011797 | Oleic acid | CID:445639 |
| 69 | IMPHY010080 | beta-Elemene | CID:6918391, |
| 70 | IMPHY007067 | Linalyl acetate | CID:8294 |
| 71 | IMPHY014988 | Limonene | CID:22311 |
| 72 | IMPHY011394 | Arachidic acid | CID:10467 |

| | | | |
|---|---|---|---|
| 73 | IMPHY014831 | beta-Caryophyllene | CID:5281515, |
| 74 | IMPHY010072 | Eucalyptol | CID:2758 |
| 75 | IMPHY006950 | Tricyclene | CID:79035, |
| 76 | IMPHY012104 | Citronellol | CID:8842 |
| 77 | IMPHY000165 | Tetracosanoic acid | CID:11197, |
| 78 | IMPHY006417 | 2,6-Dimethyl-2,4,6-octatriene | CID:5368821 |
| 79 | IMPHY007212 | Docosanoic acid | CID:8215, |
| 80 | IMPHY003485 | Myrcene | CID:31253 |
| 81 | IMPHY004631 | Stearic acid | CID:5281 |
| 82 | IMPHY007327 | Palmitic acid | CID:985, |
| 83 | IMPHY008910 | Hentriacontane | CID:12410, |

### 2.2 Molecular docking analysis

Before molecular docking analysis, the selected compounds against the alpha-amylase active site, for which the target protein and the ligands were prepared using the Protein Preparation Wizard (PrepWizard) and LigPrep Module of Schr€odinger suite[11], respective. The protein was prepared by adding the missing residues and assigning the formal and partial charges to the structure. The native ligands and the co-crystallized water molecules were deleted from the protein structure to allow the docking of new ligands into the active catalytic pocket.and the ligand was pre-proceed using the default parameters of the LigPrep module in the Schro¨dinger suite[12] , the ligands were prepared by generating their tautomeric confirmations with OPLS3e force field and EPIK state penalty at pH 7.0±2.0. A variety of software tools are available for molecular docking purpose. In this study Glide XP programs of schrodinger suit package was used for molecular docking experiment. Following molecular docking, the drug-likeness analysis for all six selected compounds was done using an online server, i.e. swissADME [13].

### 2.3 Molecular dynamics simulations

After the molecular docking, we performed a molecular dynamics simulation of the protein-ligand complex to evaluate the complex stability, protein-ligand complex was simulated further using the Desmond-maestro 2020–4 academic package[14], and every docked complex was placed in a 10 Å × 10 Å × 10 Å orthorhombic box, solvated with water (TIP4P: transferable intermolecular potential 4 points) solvent using a system builder module. Salt was added at a 0.15 M concentration to simulate physiological conditions. Later, the system was neutralized using Na+ and Cl− ions. the simulation system was minimized under default parameters using a minimization tool and subjected to 100 ns simulation under OPLS-2005 force field at 310 K temperature and 1.01325 bar pressure with default parameters using the Molecular dynamics simulation tool of free academic Desmond-maestro 2020-4[15,16].

## 3.0 Result and discussion:

### 3.1. Molecular docking and interaction analysis

The total 83 compounds of *Abrus precatorius* was docked with target proteins. Resulted in the identification of six top most active compounds was docked with alpha-amylase protein, based on their high negative docking score, namely, Vitexin(-10.6kcal/mol), delphinidin-3-5,diglucoside(-10.5kcal/mol,), abrusin(-9.18kcal/mol), taxifolin-3-glucoside (-8.83 kcal/mol), pelargonidin3-glucoside (-8.72 kcal/mol), and Quercetin (-8.22 kcal/mol ). All the selected docking score more negative than the control ligand, i.e. Myricetin (–7.3kcal/mol). The 3D and 2D figures were generated using the Free Maestro v12.3 version's Graphic User Interface. The three-dimensional and two-dimensional (3D and 2D) interaction figures were showed (Figure 1). Intermolecular interaction (IMI) analysis is performed to observe molecular interactions between the target proteins and acive compounds. This analysis revealed the formation of various non-covalent interactions such as hydrogen bonds (HBond), hydrophobic and hydrophilic (Polar) interactions, and positive and negative interactions, along with the glycine interactions between the protein and ligands in each docked complex showed in (Table-2). The IMI analysis of the docked docked complex Vitexin revealed six hydrogen bonds with the Hip[305], Glu[233], Asp[300], Arg[195], and Gln[63] residues of the target protein. Gln[63] formed one-one hydrogen bonds with the ligand, whereas Hip[305], Glu[233], Asp[300], Arg[195]formed two hydrogen bonds. While hydrophobic interactions were observed in seven residues: Ile[235], Ala[198,] Trp[58], Trp[59], Leu[162], Tyr[62], and Leu[165] .Tyr[62] also demonstrated pi-pi stacking. (figure-1(a,b)). In the case of docked complex delphinidin-3-5,diglucoside generated ten hydrogen bonds with the target protein residues Arg[195], Gln[63], Trp[59], Tyr[62], Asp[300], Ash[197], Asn[298], Lys[200], Gly[306], Glu[240]. Additionally, the hydrophobic interaction was identified by a total eleven residues Phe[256],

Leu[165], Ile[235], Ala[198], Ala[307], Trp[58], Trp[59], Leu[237], Leu[162], Tyr[62], Tyr[151] (figure-1(c,d)). Whereas, the result of the docked complex abrusin revealed six hydrogen bonds with the target protein residues Asp[300], Thr[163], Arg[195], Glu[233], Gln[63], where Thr[163], Arg[195], Glu[233], Gln[63] formed only one-one hydrogen bond with the ligand and Asp[300] formed two hydrogen bonds. While, six hydrophobic interaction formed residues Leu[165], Ala[198],Trp[58], Trp[59], Leu[162], Tyr[62] (figure-1(e,f)). Likewise, in the docked complex taxifolin-3-glucoside containing three hydrogen bonds with the target protein by active residues Asp[300], Hip[305], His[201] with the ligand . while, nine Hydrophobic interaction residues Ile[235], Ala[307], Leu[165], Ala[198], Trp[58], Trp[59], Leu[162], Tyr[62], Tyr[151](figure-1(g,h)). The result of fifth high strong docked complex pelargonidin3-glucoside displayed three hydrogen bonds with the target protein residues Tyr[151], His[201], Asp[197] formed one-one hydrogen bonds. Additionally, total eight residues Leu[165], Ala[198], Trp[58], Trp[59], Leu[162], Tyr[62], Tyr[151], Ile[235] formed the hydrophobic interaction . Along with, Trp[59] were showing pi-pi stacking (figure-1(I,j)). In the case of docked complex Quercetin displayed two hydrogen bonds with the target protein residues Gln[63], Arg[195] formed one-one hydrogen bond and total seven residues Leu[165], Ala[198], Trp[58], Trp[59], Leu[162], Tyr[62], Ile[235] discovered the hydrophobic interaction. while, Trp[59] was showing pi-pi stacking (figure-1(k,l)). In addition, the IMI analysis was also done for the control compound, i.e. Myricetin. This complex formed four hydrogen bonds with the target protein residues Asp[300], Hip[305], Tyr[62], and Asp[356]. While, total six residues Trp[357], Trp[58], Trp[59].Leu[162], Tyr[62], and Leu165 discovered the hydrophobic interaction. Along with, Trp[59] also showed pi-pi stacking (figure-1(m,n)). Concluding the overall IMI analysis results suggested that all identified compounds occupied the active catalytic pocket and interacted with similar amino acid residues of the target protein. However, all the compounds show best docking score and interaction compared to the control compound, i.e. Myricetin, indicating their higher affinity with the target protein. hence above described the top six compounds IMI analysis but the top two complexes considered for the molecular dynamics simulation studies.

| 3D Structure | 2D Structure |
|---|---|
| **(a)** 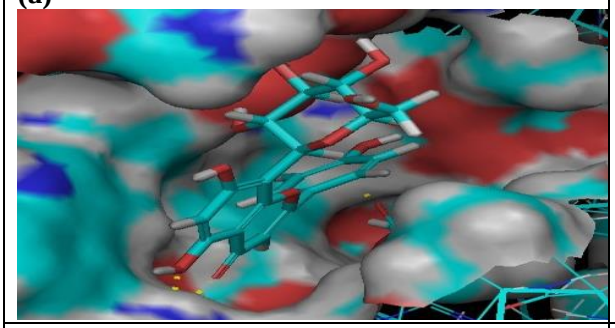 | **(b)** 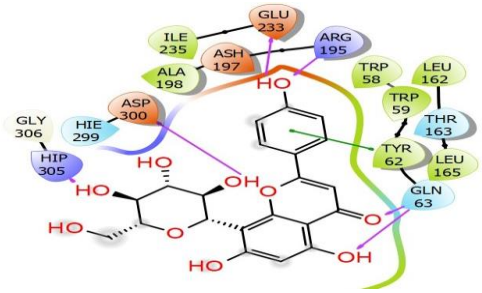  |
| **(c)** 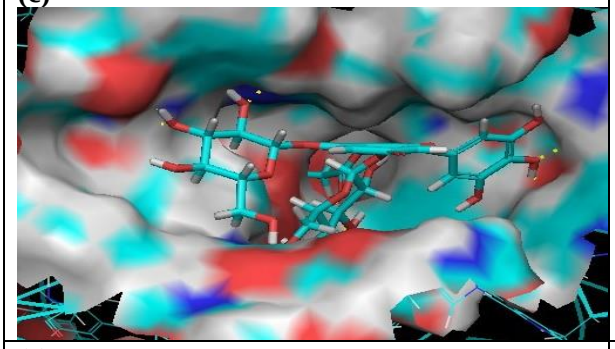 | **(d)** 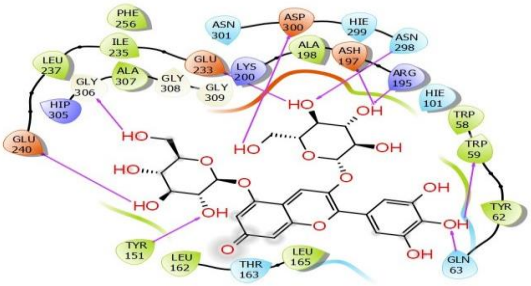  |
| **(e)** 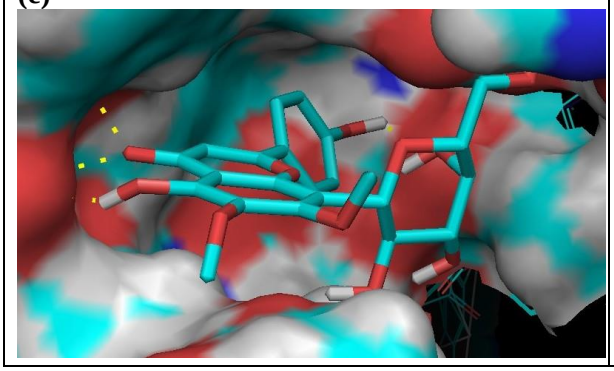 | **(f)** 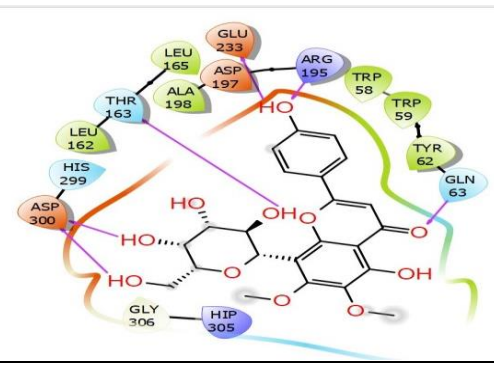  |

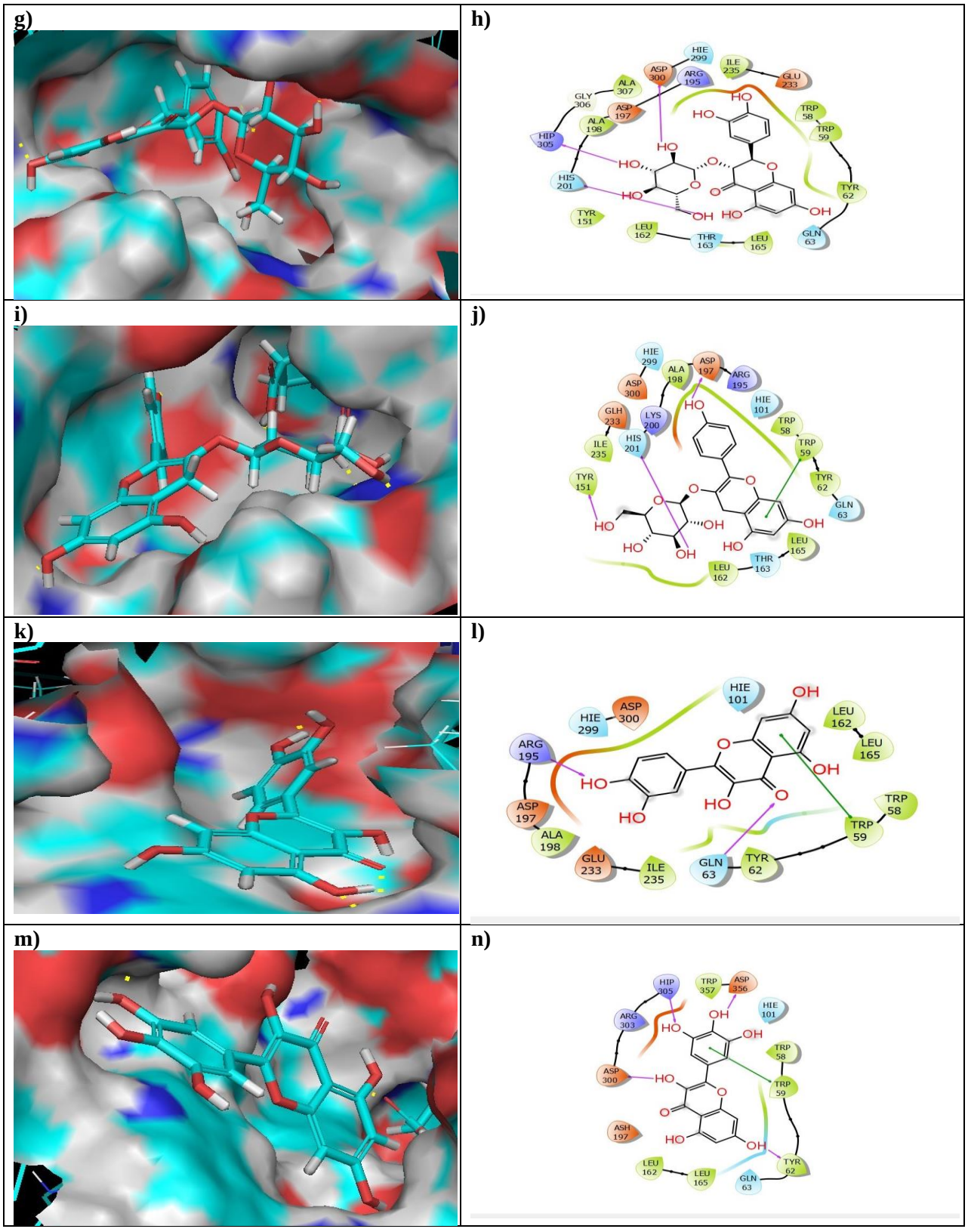


**Fig:1** 3D and 2D poses of the selected natural compounds of *Abrus precatorius*, i.e, (a,b) Vitexin, (c,d) delphinidin-3-5,diglucoside, (e,f) abrusin (g,h) taxifolin-3-glucoside,(i,j) pelargonidin3-glucoside,(k,l) Quercetin (m,n) and control i.e myricetin (m,n). In 2D interaction maps, pink arrow (H-bond), green line (π-π stacking), red-violet (salt bridge), red (negative), violet (positive), green (hydrophobic), and blue (polar) colour residues exhibits the interactions in the respective docked complexes.

**Table 2.** Intermolecular interactions were observed for the selected compounds against the Pancreatic alpha-amylase with in the respective binding pocket.

| S.No. | Complex | bond H | Hydrophobic | Polar | πstacking | Glycine | Negative | Positive |
|---|---|---|---|---|---|---|---|---|
| 1. | Vitexin | Hip$^{305}$, Glu$^{233}$, Asp$^{300}$, Arg$^{195}$, and Gln$^{63}$ | Ile$^{235}$, Ala$^{198,}$ Trp$^{58}$, Trp$^{59}$, Leu$^{162}$, Tyr$^{62}$, and Leu$^{165}$ | Hie$^{199}$ ,Thr163, Gln$^{63}$ | Tyr$^{62}$ | Gly306 | Asp$^{300}$,Ash$^{197}$, Glu$^{233}$ | Hip$^{305}$, Arg$^{19}$ |
| 2. | delphinidin-3-5,diglucoside | Arg$^{195}$, Gln$^{63}$, Trp$^{59}$, Tyr$^{62}$, Asp$^{300}$, Ash$^{197}$, Asn$^{298}$, Lys$^{200}$, Gly$^{306}$, Glu$^{240}$ | Phe$^{256}$, Leu$^{165}$, Ile$^{235}$, Ala$^{198}$, Ala$^{307}$, Trp$^{58}$, Trp$^{59}$, Leu$^{237}$, Leu$^{162}$, Tyr$^{62}$, Tyr$^{151}$ | Thr$^{163}$,Gln$^{63}$,Hie$^{101}$,Asn$^{298}$,Hie$^{299}$,Asn$^{301}$ | | Gly$^{306}$,Gly$^{308}$,Gly$^{309}$ | Glu$^{240}$,Glu$^{233}$,Asp$^{300}$,Ash$^{197}$ | -Hip$^{305}$,Lys$^{200}$,Arg$^{195}$ |
| 3. | Abrusin | Asp$^{300}$ , Thr$^{163}$ , Arg$^{195}$ , Glu$^{233}$ , Gln$^{63}$ | Leu$^{165}$ , Ala$^{198}$,Trp$^{58}$, Trp$^{59}$ , Leu$^{162}$, Tyr$^{62}$ | His$^{299}$,Thr$^{163}$,Gln$^{63}$ | | | Asp$^{300}$,Asp$^{197}$,Glu$^{233}$ | Hip$^{305}$,Arg$^{195}$ |
| 4. | taxifolin-3-glucoside | Asp$^{300}$ , Hip$^{305}$, His$^{201}$ | Ile$^{235}$, Ala$^{307}$, Leu$^{165}$ , Ala$^{198}$, Trp$^{58}$, Trp$^{59}$ , Leu$^{162}$, Tyr$^{62}$ , Tyr$^{151}$ | His$^{299}$,Thr$^{163}$,Gln$^{63}$ | | Gly$^{306}$ | Asp$^{300}$,Asp$^{197}$,Glu$^{233}$ | Hip$^{305}$,Arg$^{195}$ |
| 5. | pelargonidin 3-glucoside | Tyr$^{151,}$ His$^{201,}$ Asp$^{197}$ | Leu$^{165}$, Ala$^{198}$,Trp$^{58}$, Trp$^{59}$ , Leu$^{162}$, Tyr$^{62}$, Tyr$^{151}$, Ile$^{235}$ | Hie$^{299}$,Hie$^{101}$,Gln$^{63}$,Thr$^{163}$ ,His$^{201}$ | Trp$^{59}$ | | Asp$^{197}$,Glh$^{233}$,Asp$^{300}$ | Lys$^{200}$, Arg$^{195}$ |
| 6 | Quercetin | Gln$^{63}$, Arg$^{195}$ | Leu$^{165}$, Ala$^{198}$, Trp$^{58}$, Trp$^{59}$, Leu$^{162}$, Tyr$^{62}$, Ile$^{235}$ | Hie$^{299}$,Hie$^{101}$,Gln$^{3}$ | Trp$^{59}$ | | Asp$^{197}$,Glu$^{233}$,Asp$^{300}$ | Arg$^{195}$ |
| 7 | Myricetin (control) | Asp$^{300}$, Hip$^{305}$, Tyr$^{62}$, and Asp$^{356}$ | Trp$^{357}$, Trp$^{58}$, Trp$^{59}$.Leu$^{162}$, Tyr$^{62}$, and Leu165 | Hie$^{101}$,Thr$^{163}$,Gln$^{63}$ | Trp$^{59}$ | | Asp$^{300}$,Asp$^{356}$,Ash$^{197}$ | Hip$^{305}$,Arg$^{303}$ |

### 3.2 ADMET analysis:

Compounds proposed as prospective therapeutic candidates must have strong biological activity while being less harmful. To validate the proposed pharmacological compounds, important criteria such as absorption, distribution, metabolism, and excretion (ADME) are suggested in (Table -3). All six compounds, namely Vitexin, delphinidin-3-5,diglucoside, abrusin, taxifolin-3-glucoside, pelargonidin3-glucoside, and Quercetin, were discovered to be non-inhibitors of several cytochromes, including CYP2D6, CYP1A2, CYP2C19 , CYP2C9, CYP2D6, and CYP3A4, which are required for drug and xenobiotic metabolism. Furthermore, the chosen compounds were impermeable to the blood-brain barrier (BBB). Vitexin, pelargonidin3-glucoside, and Quercetin were all anticipated to have decreased gastrointestinal absorption. Except for delphinidin-3-5,diglucoside, abrusin, and taxifolin-3-glucoside, which violated Lipinski's rule of five by showing 3, 2, 2 respectively.The other three compounds demonstrated one violation of Lipinski's rule of five. However, the druglikeness principles do not have to be followed by natural substances because cells identify bioactive compounds by active transport[17,18]. Additionally, the ADME study recommended the selected active compounds against human pancreatic alpha-amylase with the best therapeutic qualities.

**Table 3.** ADMET profiling, Docking score and structural details of selected compounds

| Complex | Binding energy | Mol.formula | Mol.weight | BBB | CYP2 D6 | CYP1 A2 | CYP2 C19 | CYP2 C9 | CYP2 D6 | CYP3 A4 | Lipinski's rule of 5 violations |
|---|---|---|---|---|---|---|---|---|---|---|---|
| Vitexin | -10.6 | $C_{21}H_{20}O_{10}$ | 432.4g/mol | No | No | No | No | No | No | No | 1 |
| delphinidin-3-5,diglucoside | -10.5 | $C_{27}H_{31}O_{17}^{+}$ | 627.5g/mol | No | No | No | No | No | No | No | 3 |
| Abrusin | -9.18 | $C_{23}H_{24}O_{11}$ | 476.4g/mol | No | No | No | No | No | No | Yes | 2 |
| taxifolin-3-glucoside | -8.83 | $C_{21}H_{22}O_{12}$ | 466.4g/mol | No | No | No | No | No | No | No | 2 |
| pelargonidin 3-glucoside | -8.72 | $C_{21}H_{21}ClO_{10}$ | 468.8g/mol | No | No | No | No | No | No | No | 1 |
| Quercetin | -8.22 | $C_{15}H_{10}O_{7}$ | 302.23g/mol | No | Yes | No | No | Yes | Yes | No | 0 |

### 3.3 Molecular dynamic analysis:

After performing docking experiment, the top two best-docked protein-ligand complexes were taken to study their conformational stability and time-dependent behavior.100ns molecular dynamics (MD) simulations of the selected top two docked complexes as attained via docking experiment were performed using DESMOND software program. The MD simulation trajectories of the respective docked complexes were statistically analyzed in terms of root mean square deviation (RMSD) (fig:2) , RMSF (fig:3) and protein-ligand interaction fraction mapping (fig:4) to understand the dynamic stability of the docked complexes. MD simulation result of top two docked complexes of *Abrus precatorius* medicinal plants have been discussed below.

#### 3.3.1 Root Mean Square Deviation (RMSD)

RMSD was computed over the whole trajectory for both protein and ligand separately to measure the equilibration stage of the protein-ligand complex. The conformational variance of less than 3Åis deemed acceptable. If there is a minimum deviation, then the lines in the RMSD plot are parallel to the X-axis. Fig 2 shows the RMSD of all screened and control compounds over the 100 ns trajectory. Protein RMSD in all cases was under <3Å, and thus it did not show any significant deviation. Control i.e myricetin showed the deviation for protein under <2Å and ligand equal to 5Å. Here, Protein RMSD were stable from the beginning of the simulation and maintained the same pattern until the end of the simulation, but Ligand RMSD exhibited most of the deviated between 0 to 20 ns up to 7Å then attained stability with minimum deviation showed 20 to 100 ns equal to 5Å **(fig2-c)**. Likewise, the stability of the protein-fit-ligands (delphinidin 3,5-diglucoside, and vitexin) was also calculated. In the case of delphinidin 3,5-diglucoside exhibited a highly stable, it attained stability in very earlier stage 0 to 20ns under 3Å. Then It deviated between 20 to 60ns up to 3Å, and then attained stability show 60 to 100ns at 3Å **(fig2-a).** Whereas, vitexin exhibited the most deviated trajectory under <5Å **(fig2-b)** . In conclusion, the dynamic stability showed both of the complex most stable then control i.e myricetin,.

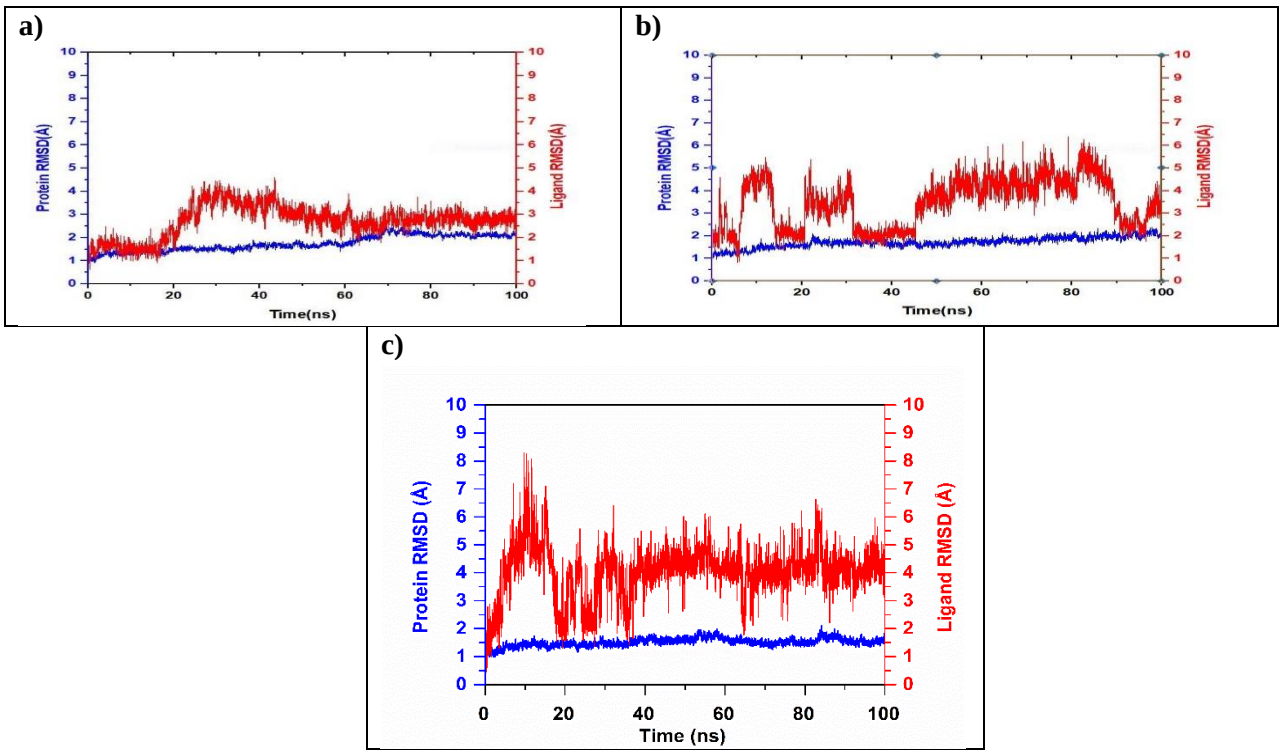


**Fig:2** Root mean square deviation (RMSD) of the receptor (blue) and ligand (red) of abrus precatorius complex a) delphinidin 3,5-diglucoside and b) vitexin and c) control compounds myricetin complex on the alpha-amylase binding site during the 100ns simulation.

### 3.3.2 Root Mean Square Fluctuation (RMSF)

Protein RMSF values were calculated for the Cα atoms of each residue. All residues from alpha-amylase showed stable RMSF < 3.5Åin all the complexes. The control compound among all the docked complexes showed the most stable pattern for all the protein residues.

The RMSF values for protein structure and residue-ligand contact mapping suggested the structural stability of human pancreatic a-amylase complexes with both the compounds compared to native ligand, i.e. Myricetin of crystal structure during 100ns simulation.

The RMSF value was also calculated for the selected compounds fitted into the binding pocket of pancreatic a-amylase with respect to the simulation time of 100ns (Fig3). In all the docked complexes, the RMSF value for all ligand atoms was in the acceptable deviation range (<3.5Å), contributing to the lower RMSD for all the selected ligands during MD simulation. The lower RMSF for the protein residues and ligand atoms in all the docked complexes suggested the overall structural stability of protein and selected ligands compared to the reference ligand, i.e. Myricetin, during the 100ns MD simulation.

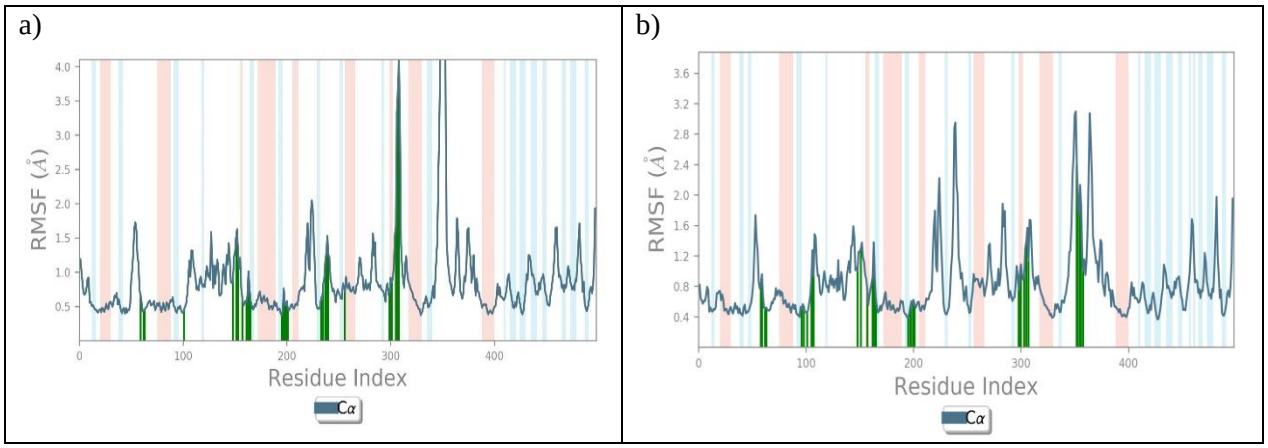

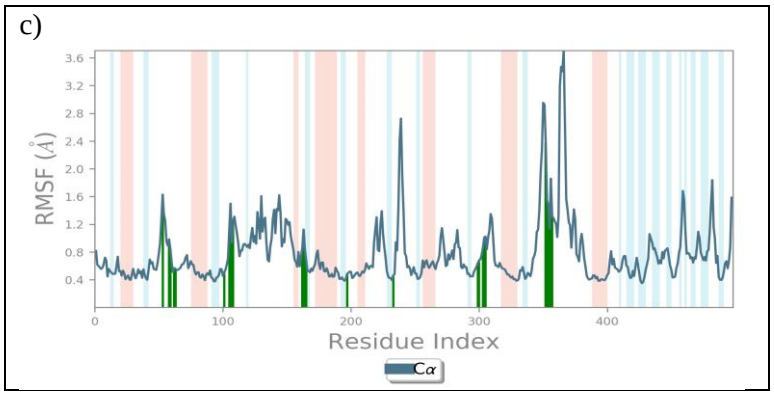


**Figure:3** Root mean square fluctuation (RMSF) plots for a) delphinidin 3,5-diglucoside and b) vitexin and c) control compounds myricetin complex with alpha-amylase Calculated over the period of 100ns molecular dynamic simulation interval.

### 3.3.3 Protein-Ligand Interaction Profiling

In the protein-ligand interaction, especially H-bond and other interactions, such as hydrophobic interaction, ionic interactions, and water bridges formation, have been reported as essential forces to maintain the stability to the complex .The Protein-Ligand Interaction of top two docked complex of alpha-amylase protein with *Abrus precatorius* complexes name (delphinidin 3,5-diglucosideE, vitexin . The Protein-Ligand Interaction Profiling of both complexes are shown in **(Fig 4).** In the case of delphinidin3,5-diglucoside docked complex exhibited residues, $Leu^{162}$, and $Leu^{165}$ formed hydrophobic interaction during the 100 ns simulation period, where $Leu^{162}$, $Leu^{165}$ showed interaction 30% and 50% of the total simulation time. Seven residues, $Tyr^{62}$, $Gln^{63}$, $His^{101}$, $Thr^{163}$, $Asp^{197}$, $Lys^{200}$ and $Glu^{240}$ formed H-Bonds, in which $Asp^{197}$ and $Glu^{240}$ showed interaction more than 100%, $Gln^{63}$ and $Thr^{163}$ interacted for only 50%, $Tyr^{62}$, $His^{101}$ and $Lys^{200}$ interacted for more than 30% of the total simulation time. Residues $Trp^{59}$ and $His^{101}$ formed both H-Bond as well as hydrophobic interaction. Water bridges were also observed significantly during the simulation formed by $Trp^{59}$ ,$Tyr^{62}$ ,$Gln^{63}$, $His^{101}$, $Ile^{148}$,$Tyr^{151}$, $Asn^{152}$ , $Arg^{161}$ , $Leu^{162}$ , $Thr^{163}$, $Arg^{195}$ ,$Ser^{199}$ , $Lys^{200}$ , $His^{201}$ $Glu^{233}$ , $Glu^{233}$ , $Ile^{235}$ ,$Glu^{240}$ , $Asp^{300}$, Asn $Arg^{303}$ ,$His^{305}$, $Asp^{356}$ and $Trp^{357}$ **(fig4-a)**. Moreover, the residues exhibiting interaction for more than 30% of the overall simulation duration were extracted from the 100ns MD simulation trajectory.$Thr^{163}$, $Glu^{240}$, $Asp^{197}$ and $Gln^{63}$ formed H-Bod, Leu165 formed hydrophobic interactions, and Gln63 also formed water bridges **(Fig5-a).** The catalytic residue $Asp^{197}$ actively participated in interactions, indicating delphinidin 3,5-diglucosideE stability within the protein active site. Interestingly, all these residues forming interaction during the simulation were also observed in the initially docked complex (Table 2).

Similarly, in the case of Vitexin docked complex residues: $Trp^{58}$, $Trp^{59}$, $Tyr^{62}$ and $Leu^{165}$ formed hydrophobic interaction. Where, $Tyr^{62}$and $Leu^{165}$ showed interaction more than 30% of the simulations time. six residues, $Trp^{59}$, $Gln^{63}$ , $His^{101}$ , $Asp^{197}$, $Asp^{300}$, $Asp^{356}$ formed hydrogen bonds, in which $Trp^{59}$, $Asp^{300}$, $Asp^{356}$ showed interaction more than 50% ,whereas, $Gln^{63}$ ,$His^{101}$and $Asp^{197}$ interacted for more than 30% of the total simulation time. Residues $Trp^{59}$ and $Trp^{58}$ formed both H-Bond as well as hydrophobic interaction. Water bridges were also observed significantly during the simulation formed by $Trp^{58}$, $Trp^{59}$,$Tyr^{62}$ ,$Gln^{63}$, $His^{101}$, $Ala^{106}$,$Tyr^{151}$,$Thr^{163}$, $Asn^{152}$, $Arg^{161}$, $Leu^{162}$, $Thr^{163}$, $Asp^{197}$, $Lys^{200}$, $His^{201}$ ,$His^{299}$, $Asp^{300}$, $Arg^{303}$ ,$His^{305}$ , $Asp^{353}$ and $Asp^{356}$ **(fig4-b).** The interaction extracted from 30% of the simulation trajectory showed residues, $Asp^{197}$ and $Trp^{59}$ formed H-Bonds for 34% and 72% of the simulation time,, whereas $Asp^{300}$ forming two H-Bonds for 44% and 46% of the total simulation time. Trp59 and Tyr62 formed hydrophobic contacts, and residue $Gln^{63}$ created a water bridge of the total simulation time **(Fig5-b)**. The catalytic residue $Asp^{197}$ showed significant interaction with the ligand during the simulation, indicating the affinity and stability of vitexin within the active catalytic site of the alpha-amylase protein. Vitexin is stability inside the active site region of the alpha-amylase protein were demonstrated by the active residue $Asp^{197}$ is strong interaction with the ligand during the simulation.

Additionally, In the case of myricetin control docked complex. Three residues, $Trp^{59}$, $His^{305}$ and $Trp^{357}$ formed hydrophobic interaction during the 100 ns simulation period, where $Trp^{59}$ and $His^{305}$ showed interaction for more than 50% of the total simulation time. Three residues, $Trp^{58}$, $Gln^{63}$, $Asp^{356}$, $His^{305}$ formed H-Bonds, in which $Trp^{58}$, $Gln^{63}$ interacted for more than 50%, whereas $Asp^{356}$ interacted for only 40% and $His^{305}$ interacted for only 10% of the total simulation time. $Trp^{59}$ and $Trp^{357}$ formed both H-Bond as well as hydrophobic interaction. The ionic interaction was also observed for a short period formed by $Asp^{356}$ and $Arg^{303}$. Water

bridges were also observed significantly during the simulation formed by Trp[59], Tyr[62], Gln63, His[101] , Ala106, Thr163, Asp197 , Asp[300] ,Arg[303] ,His[305] , Asp[356] and Trp[357]**(fig4-c).** Interestingly, the catalytic residues were present in the initially docked complex but were not observed in interactions during the simulation. The interaction profiles extracted at 30% of the total simulation period showed that residues Trp[59] and His[305] formed p-p stacking for 67% and 40%, whereas Trp[58] and Asp[356] formed H-Bonds for 72% and 49% of the total simulation period **(fig5-c).**

In the case of all docked complexes, the stability of both compounds within the active site of alpha-amylase is indicated. Furthermore, all ligands interacted with one of the catalytic residues (Asp197) of the target alpha-amylase protein, indicating that all ligands have affinity for the protein catalytic site.

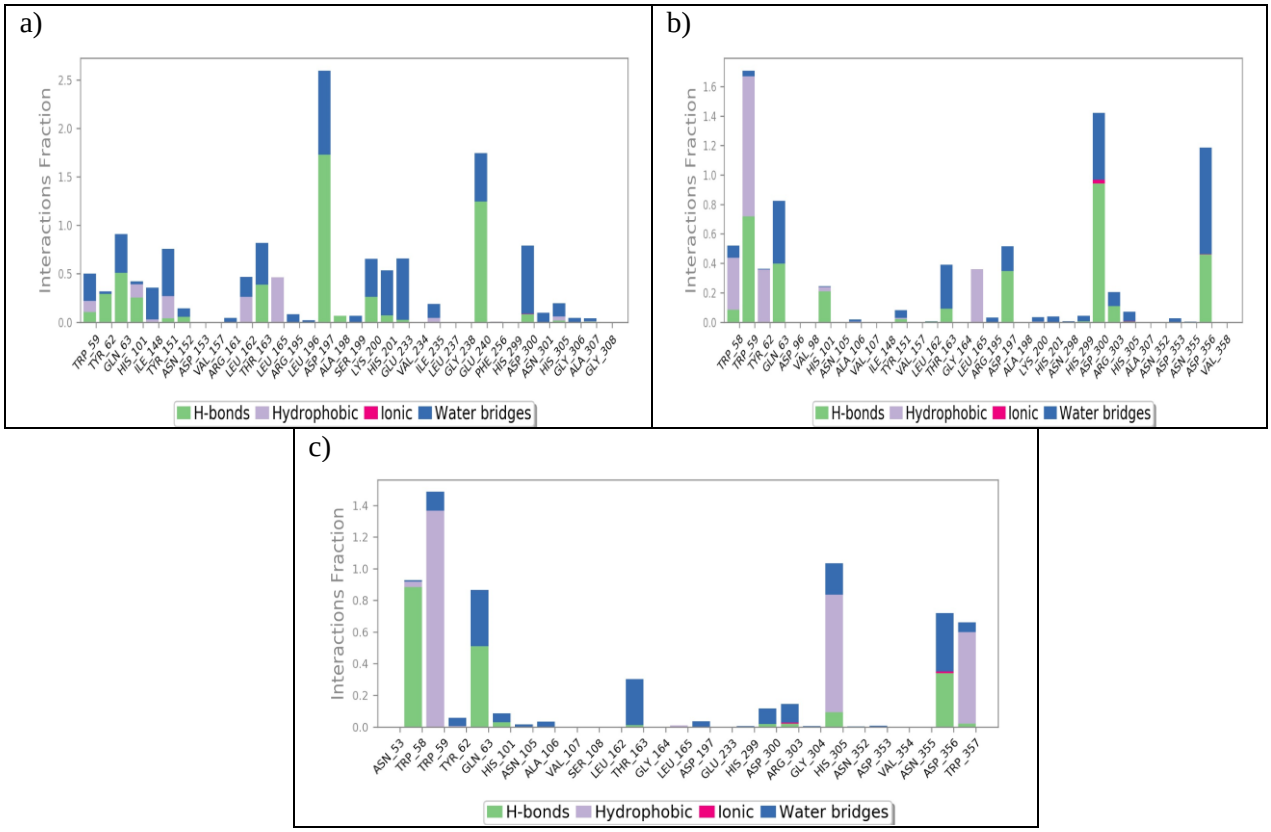


**Fig:4** Protein-ligand contact mapping of ( a) delphinidin 3,5-diglucoside, b) vitexin), and control compound g) myricetin on the alph-amylase binding site during the 100ns simulation.

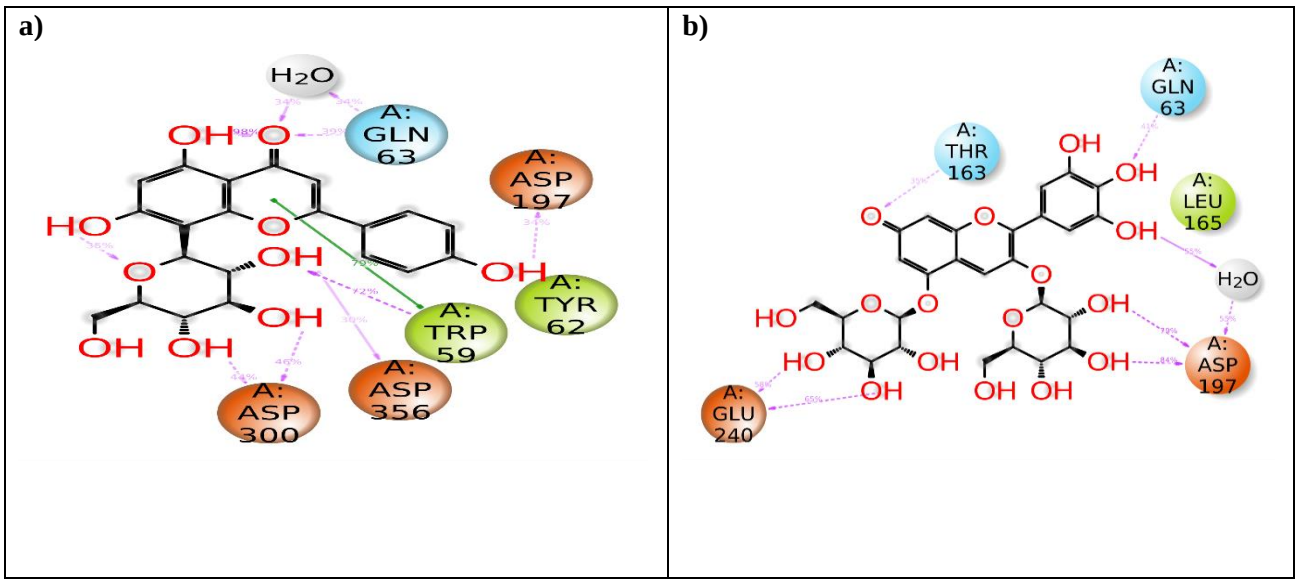

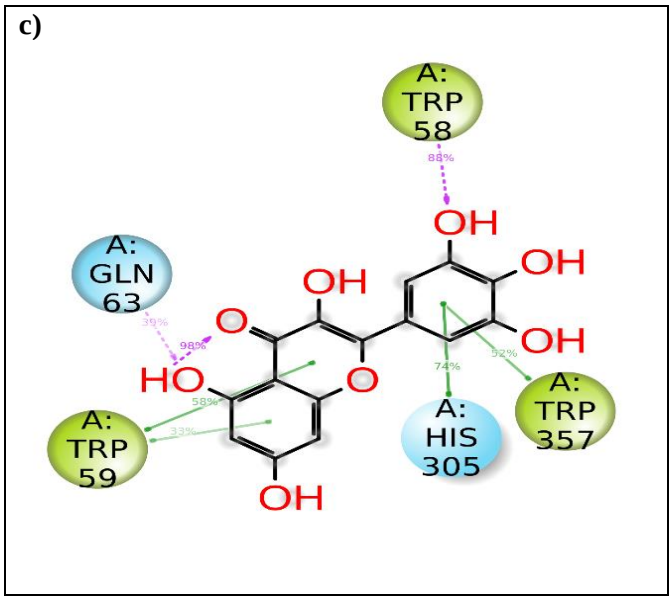


**Figure 5.** 2D interaction Diagrams of Ligand-Protein contact for selected compounds of ( a) delphinidin 3,5-diglucoside, b) vitexin), and control compound g) myricetin on the alph-amylase binding site during the 100ns simulation.

**4. Conclusion:**

In silico molecular docking of 83 compounds of *Abrus precatorius* derived resulted in the identification of the six best compounds with high negative docking scores, viz., Vitexin(-10.6kcal/mol), delphinidin-3-5,diglucoside(-10.5kcal/mol,), abrusin(-9.18kcal/mol), taxifolin-3-glucoside (-8.83 kcal/mol) , pelargonidin3-glucoside (-8.72 kcal/mol), and Quercetin (-8.22 kcal/mol). All the docking score more negative than the control ligand, i.e. Myricetin (–7.3kcal/mol) . The docking and interaction analysis revealed that all selected compounds interacted with either one of the catalytic ($Asp^{197}$) or other accessory residues of the protein 's catalytic site. The most stable trajectory was exhibited by delphinidin-3-5,diglucoside (< 3.0Å RMSD) and vitexin (<5.0Å RMSD). Based on molecular docking and dynamic simulation research, As a result, Both compounds shown substantial affinity and stability with the active site of pancreatic a-amylase and Both compounds found in this study are proposed as promising antidiabetic possibilities and should be further investigated for in vitro and in vivo confirmation..

**Reference:**

1. Alex B. ,Victor Y.A.B ,Desmond O. A. ,and Eric G. O., *Abrus precatorius* Leaf Extract Reverses Alloxan/NicotinamideInduced Diabetes Mellitus in Rats through Hormonal (Insulin, GLP-1, and Glucagon) and Enzymatic (α-Amylase/αGlucosidase) Modulation, BioMed Research International ,Article ID 9920826, 17 pages (2021).
2. Pratistha S.,Vinay K.S., Anil K.S, Molecular docking analysis of candidate compounds derived from medicinal plants with type 2 diabetes mellitus targets, Bioinformation 15(3): 179-188 (2019).
3. Madhusudhana R. I. , Dharma T. N. , Bhagvan M. R. , Pavan k.R , Gupta A. , Sarva R.C. A.S.R., antidiabetic activity of the seeds of abrus precatorius in streptozotocin & nicotinamide induced diabetic rats. pharmacologyonline 1: 701-705 (2010).
4. Ali S. A., Syed H., Md Tabish R. , Ali A. E. , Shaza Al-M. , Valentina R., Mohammed S. A., Rabab A. E. and Mohamed F.A., Alpha-Amylase and Alpha-Glucosidase Enzyme Inhibition and Antioxidant Potential of 3- Oxolupenal and Katononic Acid Isolated from *Nuxia oppositifolia, Biomolecules*, ,10( 61):591 - 13( 2020).
5. Sindhu. S. N., Vaibhavi K. and Anshu M., *In vitro* studies on alpha amylase and alpha glucosidase inhibitory activities of selected plant extracts , European Journal of Experimental Biology, 3(1):128-132 (2013) .

6. Ninon G. E. R. E., Jelili A. B., Jeanine L. M., Emmanuel I. I., Felix N., and Ahmed A. H., Alpha-Glucosidase and Alpha-Amylase Inhibitory Activities, Molecular Docking, and Antioxidant Capacities of Salvia aurita Constituents, Antioxidants, 9(1149):1-14 (2020).
7. Vinay S., Chandan D., Sushma P., Anisha S J., Shiva P.K., Bindya S,C. S., Sharanagouda S P., Ashwini P., Chandan S., *In-Silico* elucidation of *Abrus precatorius* phytochemical against *Diabetes mellitus* , Bull. Env. Pharmacol. Life Sci., 10(4):118-128(2021).
8. Berman H.M., Westbrook, J., Feng, Z., Gilliland, G., Bhat T.N., Weissig H., Shindyalov I.N., Bourne P.E., The protein data bank. Nucleic Acids Res, (28):235–242(2000). (https://www.rcsb.org/,)
9. Mohanraj K., Karthikeyan B. S., Vivek A.R.P., Chand R. P. B., Aparna, S. R., Mangalapandi P., & Samal A. IMPPAT: A curated database of Indian medicinal plants, phytochemistry and therapeutics. Scientific Reports, 8(1):4329(2018). https://doi.org/10.1038/s41598-018-22631-z
10. Kim, S., Thiessen, P.A., Bolton, E.E., Chen, J., Fu, G., Gindulyte, A., Han, L., He J., He S., Shoemaker B.A., et al. PubChem substance and compound databases. Nucleic Acids Res., (44):D1202–D1213 (2016). https://doi.org/10.1093/nar/gkv951
11. Madhavi S. G., Adzhigirey, M. D.T., Annabhimoju, R., & Sherman, W. Protein and ligand preparation: Parameters, protocols, and influence on virtual screening enrichments. Journal of Computer-Aided Molecular Design, 27(3):221–234(2013). https://doi.org/10.1007/s10822-0139644-8
12. Schr€odinger. (2018). Schr€odinger Release 2018-3: LigPrep. Schrodinger, LLC.
13. Daina, A., Michielin, O., & Zoete, V.,SwissADME: A free web tool to evaluate pharmacokinetics, drug-likeness and medicinal chemistry friendliness of small molecules. Scientific Reports, 7(1): 42717(2017). https:// doi.org/10.1038/srep42717
14. Bowers KJ, Chow DE, Xu H, Dror RO, Eastwood MP, Gregersen BA, et al. Scalable Algorithms for Molecular Dynamics Simulations on Commodity Clusters. ACM/IEEE SC 2006 Conference (SC'06). Tampa, FL: IEEE, (72): 43–43((2006).
15. Schro¨dinger Release 2020–4: Desmond Molecular Dynamics System, D.E. Shaw Research: New York, NY,Maestro-Desmond Interoperability Tools; Schro¨dinger: New York, NY, USA, 73(2020).
16. Virendra P.T., Amit D., MohammedAl-S, & Indra P.T., Exploration of human pancreatic alpha-amylase inhibitors from Physalis peruviana for the treatment of type 2 diabetes, Journal of Biomolecular Structure and Dynamics,1-17(2023).
17. Lipinski, C. A. , Lead- and drug-like compounds: The rule-of-five revolution. Drug Discovery Today. Technologies, 1(4):337–341 (2004). https:// doi.org/10.1016/j.ddtec.2004.11.007
18. Macarron, R. ,Critical review of the role of HTS in drug discovery. Drug Discovery Today, 11(7–8):277–279(2006).https://doi.org/10.1016/j.drudis.2006.02.001